



# Inundation depth affects ecosystem CO<sub>2</sub> and CH<sub>4</sub> exchange by changing plant productivity in a freshwater wetland in the Yellow River Estuary

Mingliang Zhao · Guangxuan Han · Haitao Wu · Weimin Song · Xiaojing Chu · Juanyong Li · Wendi Qu · Xinge Li · Siyu Wei · Franziska Eller · Changsheng Jiang

Received: 26 January 2020 / Accepted: 16 June 2020  
© Springer Nature Switzerland AG 2020

## Abstract

**Aims** Climate change (extreme rainfall) and water management activities have led to variation in hydrological regimes, especially inundation, which may alter the function and structure of wetlands as well as wetland-atmosphere carbon (C) exchange. However, the degree to which different inundation depths (standing water depth above the soil surface) affect ecosystem CH<sub>4</sub> fluxes, ecosystem respiration (R<sub>eco</sub>) and net ecosystem CO<sub>2</sub> exchange (NEE) remains uncertain in wetland ecosystems.

**Methods** We conducted a field inundation depth manipulation experiment (no inundation, i.e. only natural precipitation; 0, water-saturated; 5, 10, 20, 30 and 40 cm inundation depth) in a freshwater wetland of the Yellow River Delta, China. The CH<sub>4</sub> fluxes, R<sub>eco</sub> and NEE were measured with a static chamber technique during the growing seasons (May–October) of 2018 and 2019.

**Results** Inundation depth significantly increased plant shoot density, above-water level leaf area index (WLAI), above-water level plant shoot height (WHeight), aboveground and belowground biomass of

## Highlights

1. Variations in ecosystem CH<sub>4</sub> and CO<sub>2</sub> exchange at different inundation depths are addressed
2. Inundation depth increased the reed density, height, leaf area index and biomass
3. Ecosystem CH<sub>4</sub> and CO<sub>2</sub> exchange exhibited parabolic responses to inundation depth
4. Plant traits correlated with ecosystem C exchange under different inundation depths
5. Inundation decreased the global warming potential during the growing season

Responsible Editor: Hans Lambers.

**Electronic supplementary material** The online version of this article (<https://doi.org/10.1007/s11104-020-04612-2>) contains supplementary material, which is available to authorized users.

M. Zhao · C. Jiang (✉)  
State Cultivation Base of Eco-agriculture for Southwest Mountainous Land, College of Resources and Environment, Southwest University, Chongqing 400715, China  
e-mail: jiangcs@126.com

M. Zhao · G. Han (✉) · W. Song · X. Chu · J. Li · W. Qu · X. Li · S. Wei  
CAS Key Laboratory of Coastal Environmental Processes and Ecological Remediation, Yantai Institute of Coastal Zone Research (YIC), Chinese Academy of Sciences(CAS), Yantai, Shandong 264003, People's Republic of China

the dominant grass *Phragmites australis* in both years. Meanwhile, inundation depth increased the CH<sub>4</sub> fluxes, R<sub>eco</sub> (except for 0 cm) and NEE compared to no inundation, which could be attributed partly to the increased plant productivity (shoot density, WLAI, WHeight, biomass). Additionally, the CH<sub>4</sub> fluxes, R<sub>eco</sub> or NEE exhibited parabolic responses to inundation depth. Furthermore, global warming potential (GWP) was significantly decreased under different inundation depths during the growing season, especially from 5 to 40 cm inundation depth in 2019. NEE was the largest contributor to the seasonal GWP, which indicates that the inundated wetlands are a net sink of C and have a cooling climate effect in the Yellow River Delta.

**Conclusions** Inundation depth substantially affects the magnitude of CH<sub>4</sub> fluxes, R<sub>eco</sub> and NEE, which were correlated with altered plant traits in wetland ecosystems. Inundation depth could mitigate greenhouse gas emissions in the *P. australis* wetlands during the growing season. Inundation depth-induced ecosystem C exchange should be considered when estimating C sequestration capacity of wetlands due to climate change and water management activities, which will assist to accurately predict the impact of hydrological regimes on C cycles in future climate change scenarios.

**Keywords** Inundation depth · Plant productivity · Net ecosystem CO<sub>2</sub> exchange · Ecosystem respiration · Ecosystem CH<sub>4</sub> fluxes

## Introduction

Wetlands occupy only 5–8% of the Earth's total land surface (Mitsch and Gosselink 2007), but are widely recognized as high-carbon (C) ecosystems in the biosphere, because wetlands hold 20–30% of the estimated

1500 Pg of the global soil C pool (Nahlik and Fennessy 2016). Therefore, wetlands play an important role in regulating the C cycle at a global scale (Xiao et al. 2019). The hydrological regime is a key process in wetland ecosystems, which not only affects the structure and function of wetland ecosystems but also controls the C sink and source of wetlands (Webb and Leake 2006; Jimenez et al. 2012; Rasmussen et al. 2018). Hydrological regimes have been altered by global climate change in terrestrial ecosystems during recent years, resulting in increases in intensity and frequency of extreme rainfall, thereby increasing the risk of prolonged inundation (IPCC 2013; Trenberth 2011; Westra et al. 2014). These alterations in hydrology (e.g. inundation) increase the likelihood of changes in wetland ecosystem structure and function, affecting ecosystem C exchange (e.g. carbon dioxide (CO<sub>2</sub>) and methane (CH<sub>4</sub>); Han et al. 2015; Sánchez-Rodríguez et al. 2019). Thus, it is important to understand how the wetland-atmosphere C exchange responds to changes in hydrological conditions, such as inundation, which may potentially pose a large feedback to ongoing climate change (Han et al. 2015; Zhao et al. 2019).

Inundation creates anaerobic conditions in the flooded soil that exert a physiological stress on wetland plants depending on the inundation-tolerance of a species (Liu et al. 2018; Zhao et al. 2018). For less inundation-tolerant plants, this stress limits photosynthetic leaf area due to partial submergence of shoots and leaves (Schedlbauer et al. 2010; Jimenez et al. 2012). At the same time, the diffusion rate of CO<sub>2</sub> in water is slower than in air (Matsuda et al. 2017), which results in reduced leaf photosynthesis due to slow uptake of CO<sub>2</sub> into leaves. In addition, the photosynthesis of submerged leaves can be limited mainly through hindering the light transmission, especially when the above surface water is deep and/or turbid (Han et al. 2015). Moreover, inundation causes an oxygen deficiency to roots and disrupts the connection with the atmosphere (Garssen et al. 2015). Consequently, anoxic conditions inhibit root respiration and plant photosynthesis, which has a negative impact on plant growth (Sairam et al. 2008). In addition to ecosystem CO<sub>2</sub> uptake, inundation may also reduce ecosystem respiration. On the one hand, inundation results in partial plant stomatal closure and transpiration cessation below the water surface and restrains plant respiration (Han et al. 2015; Zhao et al. 2019) and microbial respiration, attributed to lowered diffusion of oxygen, limited aerobic microbial activity,

M. Zhao · G. Han · W. Song · X. Chu · J. Li · W. Qu · X. Li · S. Wei  
Shandong Key Laboratory of Coastal Environmental Processes, YICCAS, Yantai, Shandong 264003, People's Republic of China

H. Wu  
Northeast Institute of Geography and Agroecology, Chinese Academy of Sciences, Changchun 130102, China

F. Eller  
Department of Bioscience, Aquatic Biology, Aarhus University, Ole Worms Alle 1, Aarhus C 8000, Denmark

C mineralization and decomposition rates (Jimenez et al. 2012; McNicol and Silver 2014). On the other hand, due to the slow diffusion rate of CO<sub>2</sub> in water, the diffusive boundary layer resistance could limit rates of CO<sub>2</sub> emission through the water surface (Han et al. 2015). Therefore, the effect of hydrological regimes on CO<sub>2</sub> uptake and emission are unequal, which can result in remarkable alterations in ecosystem C balance.

Wetlands often act as a net source of CH<sub>4</sub>, especially wetland ecosystems that are inundated to a high degree, which is strongly related to the higher activity of methanogenic bacteria, lower oxidation rates and transport of CH<sub>4</sub> from the anaerobic zone to the atmosphere (Cheng et al. 2007; Koelbener et al. 2010; Bridgham et al. 2013). On the one hand, inundation could promote inundation-tolerant plant growth, such as *Phragmites australis* and *Typha domingensis*, which provide organic substrates for methanogens by biomass decomposition and root exudation, consequently enhancing CH<sub>4</sub> emissions in a flooded, anaerobic environment (Cheng et al. 2007; Koelbener et al. 2010; Yang et al. 2013). Moreover, these vascular plants can transport CH<sub>4</sub> from the root zone to the atmosphere through dead culms, thereby bypassing the oxidizing layers and enhancing CH<sub>4</sub> emissions. On the other hand, aerenchyma of vascular plants can transport O<sub>2</sub> to the rhizosphere and promote the oxidation of CH<sub>4</sub> in a micro-aerobic environment under inundated conditions (Henneberg et al. 2012; Bridgham et al. 2013).

However, there are only a few studies on the effects of inundation on ecosystem CO<sub>2</sub> and CH<sub>4</sub> exchange in different types of wetlands, and the outcomes from these studies are conflicting. For example, inundation weakened the ecosystem CO<sub>2</sub> sink and ecosystem respiration strength in a Florida Everglades marsh with a short-hydroperiod (Schedlbauer et al. 2010; Zhao et al. 2019) and in a supratidal wetland of the Yellow River Delta (Han et al. 2015). On the contrary, inundation increased ecosystem CO<sub>2</sub> sink, respiration and CH<sub>4</sub> fluxes with increasing vegetation biomass in a temperate fen after inundation (Minke et al. 2016). Although many studies have focused on the effects of hydrological conditions (especially groundwater table) on ecosystem CO<sub>2</sub> and CH<sub>4</sub> exchange in different wetlands (Jungkunst and Fiedler 2007; Olefeldt et al. 2017; Ratcliffe et al. 2019; Wang et al. 2017; Yang et al. 2014), less effort has been conducted to understand the effect of inundation intensity and especially different inundation depths. This suggests that more

investigations are required to elucidate the regulatory mechanisms governing the influence of inundation depths on ecosystem CO<sub>2</sub> and CH<sub>4</sub> exchange in wetland ecosystems.

The Yellow River Delta is one of the most active regions of land-ocean interaction among the many river deltas in the world. The interaction of groundwater, precipitation and seawater intrusion has produced a variety of wetland types, plant communities, and ecological functions under different hydrological conditions (Han et al. 2015). During the rainy season, different inundation depths are observed, which depend on the intensity of precipitation. In recent years, the frequency and intensity of extreme rainfall have increased (Han et al. 2018), which indicates that the inundation frequency of wetlands is also increasing. Furthermore, the Chinese government has used freshwater from the Yellow River to restore the degraded wetlands in the Yellow River Delta wetlands in the past 20 years (Yang et al. 2017), which also caused more wetland soils to be inundated. These changes in inundation depth caused by extreme rainfall and water management activities may modify wetland-atmosphere CO<sub>2</sub> and CH<sub>4</sub> exchange. Therefore, we conducted a field inundation depth manipulation experiment in a freshwater wetland in the Yellow River Estuary during the growing season in 2018 and 2019. Our objectives were (1) to understand how changes in inundation depth affects plant traits and (2) to illustrate how ecosystem CO<sub>2</sub> and CH<sub>4</sub> exchange respond to changes in inundation depth.

## Materials and methods

### Site description

This study was carried out in the Yellow River Delta Ecological Research Station of Coastal Wetland (37°45' 50" N, 118°59'24" E, elevation: ~2.5 m above sea level), Chinese Academy of Sciences, which is located in Kenli County, Shandong Province, China. The site is located in supratidal wetlands of the Yellow River Delta. It has a warm-temperate and continental monsoon climate. The mean annual temperature is 12.9 °C. Annual precipitation averages 550–640 mm, ~74% of which occurs from June to September. After extreme rainfall, the wetlands are often inundated to different water levels, which will last for nearly 1–2 months. During the extreme rainfall-driven inundation, the

cumulative rainfall reached nearly 230 and 300 mm in 2018 and 2019, respectively (the weather data comes from the research station). The hydrology of the site is affected by the interactions of groundwater, precipitation and seawater. Meanwhile, the hydrology of the region is influenced by the use of freshwater from the Yellow River (Yang et al. 2017) to restore degraded wetlands in the Yellow River Delta National Nature Reserve. The groundwater table is shallow with an average depth of 1.14 m. The soil type gradually varies from fluvo-aquic to saline soil, and soil texture is mainly sandy clay loam with  $6.54 \text{ g kg}^{-1}$  soil organic matter content at 0–20 cm depth. The vegetation is relatively homogeneous and strongly dominated by common reed (*Phragmites australis*) with other associated species including *Suaeda salsa*, *Tamarix chinensis*, *Imperata cylindrica*, and *Tripolium vulgare*.

### Experimental design

The experiment consisted of seven soil surface inundation depths, including control (no inundation, only natural precipitation, CK), 0 (water-saturated), 5, 10, 20, 30 and 40 cm inundation depth, respectively. Each treatment was replicated four times, and each replicate plot (2 m length  $\times$  2 m width  $\times$  0.5 m height) was separated by cement barriers at a 40 cm distance. Soil and vegetation were rarely damaged during installation of the cement barriers. There was an opaque plastic water tank (80 cm diameter and 120 cm long) at the position of 1.5 m above the ground connected to each plot with tubes. The float ball, installed at the end of the tube, controlled the water level in each plot. When the water levels fell, the valve body would sink down and the water would flow into the plot. The water could not be stopped until the water level reached the fixed inundation depth (Fig. S1). The water came from a small lake (below  $1 \text{ mS cm}^{-1}$ ) near the experimental site (originally from the Yellow River which runs into the Bohai Sea) and a pump was used to pump the water into the tank after filtration to prevent the inflow of large particles and algae into the tank and tubes. There was a small hole in the wall of each plot, which was used to drain the excess water out of the plot after rain. The inundation treatments were applied from April to October of each year starting in 2017 and the vegetation of each plot was dominated by *P. australis*.

### Measurements of ecosystem $\text{CO}_2$ and $\text{CH}_4$ exchange

The ecosystem C exchanges including net ecosystem  $\text{CO}_2$  exchange (NEE), ecosystem respiration ( $R_{\text{eco}}$ ) and  $\text{CH}_4$  fluxes were all measured with an LGR Ultraportable Greenhouse Gas Analyzer (UGGA, Los Gatos Research, Inc., San Jose, USA) that measures gas concentrations continuously and automatically. The LGR analyzer was attached to transparent (NEE,  $\text{CH}_4$  flux) and opaque ( $R_{\text{eco}}$ ) cylindrical chambers (Plexiglas), which were put over patches covered by *P. australis* inside each plot. The static chambers consisted of transparent acrylic plastic with three parts: a base frame (30 cm in diameter, 10, 10, 15, 20, 30, 40, 50 cm in height for the seven treatments, respectively), a removable middle box (30 cm in diameter, 100 cm in height) and a removable top box (30 cm in diameter, 100 cm in height). The base frames were installed into the soil to 5 cm depth, with 5 cm of the frame emerging above the water surface (Wei et al. 2020), in the center of each plot in May 2018. The removable middle box was only used when the height of the vegetation was higher than 100 cm. The removable middle or top box was carefully placed on the top of the base frame and sealed with a sealing strip at the joints in order to maintain the chamber sealed during the measurement. Two battery driven fans (8 cm in diameter, 12 V) were installed inside the top of each chamber to generate turbulence inside the chamber during sampling. The gas fluxes (NEE,  $R_{\text{eco}}$ ,  $\text{CH}_4$  flux) were measured once a month in 2018, twice a month in 2019 (from 8:00 a.m. to 11:00 a.m.) during the growing season (from May to October). For each measurement, chambers were sealed for 3 min, and  $\text{CO}_2$  and  $\text{CH}_4$  fluxes were measured.

### Measurements of shoot density, WLAI, WHeight, biomass

During the growing season, above-water level leaf area index (WLAI) of *P. australis* was measured using an ACCUPAR LP-80 ceptometer (METER Group, Pullman, WA, USA). Because the LAI is dependent on the spatial and illumination characteristics of the scanned location, four scans were made for each plot in the four cardinal directions. Consequently, the average of the four measurements was considered as the WLAI value for each plot. In addition, we measured the *P. australis* density and above-water level height (WHeight) per  $\text{m}^2$  in the plots when measuring the ecosystem  $\text{CH}_4$  fluxes,

$R_{\text{eco}}$ , and NEE. The biotic factors were measured once a month in 2018 and twice a month in 2019. Before biomass harvest, the water in each plot was removed. Aboveground biomass (AGB) was clipped at the sediment surface from a 0.25 m<sup>2</sup> quadrat in each plot, oven dried at 65 °C for at least 2 days until no weight loss occurred anymore, and weighed. One soil core (10 cm in diameter) of 0–40 cm was excavated in each plot. The root samples from the core were washed by wet sieving under gently flowing water to remove attached soil and debris, then oven dried at 65 °C for 2 days, and weighed to determine the belowground biomass (BGB).

### Global warming potential (GWP)

In the estimation of GWP, CO<sub>2</sub> is used as a reference gas. The CH<sub>4</sub> emissions are converted to the equivalent amounts of CO<sub>2</sub> based on the GWP value. The growing season CH<sub>4</sub> emission was converted to CO<sub>2</sub> equivalents by multiplying with a GWP factor of 28 (based on a 100-year time horizon). A positive GWP indicates a release of greenhouse gases (GHGs) to the atmosphere and a potential climate warming effect, while a negative GWP indicates GHG uptake from the atmosphere and a potential climate cooling effect (Tian et al. 2015). We calculated the GWP of the different inundation depths by using the following equation (IPCC 2013):

$$\text{GWP}(\text{CO}_2\text{equivalent}) = \text{CO}_2 \times 1 + \text{CH}_4 \times 28$$

### Statistical analysis

In each year, NEE,  $R_{\text{eco}}$ , CH<sub>4</sub> fluxes, GWP and biotic factors (shoot density, WLAI, WHeight, AGB and BGB) were subjected to one-way ANOVA and significant differences between different inundation depths were examined with the Turkey's multiple range test. Multiple regressions were performed for the relationships between seasonal mean CH<sub>4</sub> fluxes,  $R_{\text{eco}}$ , NEE and inundation depth or biotic factors under different inundation depths. Two-way analysis of variance (ANOVA) was conducted to analyze the NEE,  $R_{\text{eco}}$ , CH<sub>4</sub> fluxes, GWP and biotic factors, including inundation depth, years and their interactions. In all tests, a significance level of 0.05 was used. Statistical analyses were

conducted using software package SPSS version 13.0 (SPSS Inc., Chicago, IL, USA).

## Results

Changes in shoot density, WLAI, WHeight and biomass under different inundation depths

Inundation depth significantly affected all biotic factors (Figs. 1 and 2 Table 1). The reed shoot density gradually increased from early April to late August, and then decreased until the end of growing season in 2018 and 2019 (Fig. S2a and b). Inundation significantly increased plant shoot density compared with the control, but there was no significant difference between the different inundation depths (Fig. 1a and b). The above-water level reed height (WHeight) gradually increased in the early growing season in 2018 and 2019, and then reached a peak in late August. After that, WHeight did not change any more (Fig. S2c and d). Inundation significantly increased WHeight relative to the control ( $P < 0.05$ ). The highest WHeight was 212.6 cm and 212.2 cm at 10 cm inundation depth and gradually decreased from 20 to 40 cm inundation depth in both years (Fig. 1c and d). The seasonal dynamics of above-water level leaf area index (WLAI) under different inundation depths showed a similar pattern throughout both growing seasons. The WLAI gradually increased in the early growing season, then reached a peak in late July. By August, WLAI decreased in all treatments as a consequence of leaf senescence (Fig. S2e and f). Inundation significantly increased WLAI compared to the control ( $P < 0.05$ ) but no significant changes in WLAI were found from 10 to 40 cm inundation depth. The highest WLAI was 3.79 and 3.94 under 20 cm inundation depth in 2018 and 2019, respectively (Fig. 1e and f). Inundation significantly increased the AGB and BGB compared to the control ( $P < 0.05$ , Table 1), but had no significant effects from 0 to 40 cm inundation depth in either year (Fig. 2). BGB accounted for 59% and 61% of total biomass in 2018 and 2019, respectively. Overall, nonlinear relationships between WHeight, WLAI, biomass and inundation depth can be observed (Figs. 1 and 2). Additionally, there was no significant difference in shoot density, WHeight, AGB and BGB between the two years

**Fig. 1** Variations in (a, b) plant density, (c, d) plant height relative to water level (WHeight) and (e, f) above-water level leaf area index (WLAI) at different inundation depths during the growing season in 2018 and 2019. Data (means  $\pm$  SE,  $n = 4$ ) followed by different letters indicate significant differences ( $P < 0.05$ )

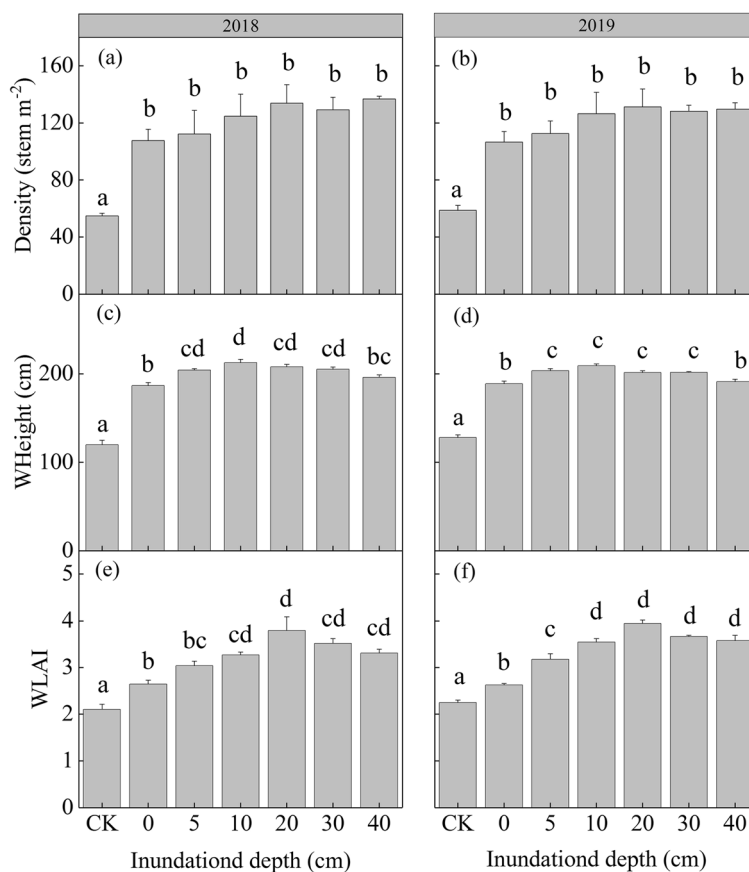


**Fig. 2** Variations in (a, b) aboveground biomass (AGB) and (c, d) belowground biomass (BGB) at different inundation depths during the growing season in 2018 and 2019. Data (means  $\pm$  SE,  $n = 4$ ) followed by different letters indicate significant differences ( $P < 0.05$ )

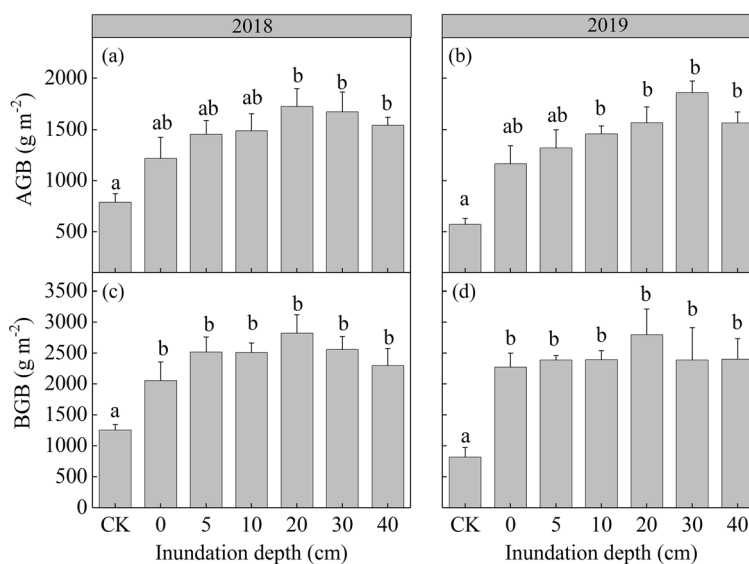


**Table 1** Results (F values) of two-way ANOVA on the effects of Inundation depth (ID), year (Y) and their interactions on plant shoot density, above-water level leaf area index (WLAI), plant height relative to water level (WHeight), aboveground biomass

| Effect | Density  | WLAI     | WHeight   | AGB     | BGB     | CH <sub>4</sub> | R <sub>eco</sub> | NEE       | GWP      |
|--------|----------|----------|-----------|---------|---------|-----------------|------------------|-----------|----------|
| ID     | 15.12*** | 54.38*** | 213.84*** | 9.36*** | 7.18*** | 26.32***        | 28.82***         | 39.26***  | 9.88***  |
| Y      | 0.02     | 6.97*    | 0.65      | 0.65    | 0.27    | 147.36***       | 61.68***         | 388.48*** | 382.8*** |
| ID × Y | 0.06     | 0.36     | 1.50      | 0.21    | 0.24    | 4.91**          | 0.74             | 9.55**    | 11.61*** |

(AGB) and belowground biomass (BGB), ecosystem CH<sub>4</sub> fluxes (CH<sub>4</sub>), ecosystem respiration (R<sub>eco</sub>), net ecosystem CO<sub>2</sub> exchange (NEE) and Global warming potential (GWP)

and no significant interactive effect between inundation depth and year (Table 1).

#### Effects of inundation depth on ecosystem CO<sub>2</sub> and CH<sub>4</sub> exchange

The CH<sub>4</sub> fluxes, R<sub>eco</sub> and NEE showed distinct seasonal patterns under different inundation depths during the growing season in 2018 and 2019 (Fig. S3). Ecosystem CH<sub>4</sub> fluxes gradually increased during the early growing season, and then reached a peak in August and rapidly declined thereafter (Fig. S3a and b). With the *P. australis* canopy fully developed, R<sub>eco</sub> and NEE reached a peak in late July in both years under the different inundation depths. From August to October, the R<sub>eco</sub> and NEE rapidly decreased with the decrease of solar radiation, temperature and WLAI (Fig. S3c–f).

Inundation depth significantly affected the magnitudes of CH<sub>4</sub> fluxes, R<sub>eco</sub> and NEE in 2018 and 2019 (Fig. 3). The CH<sub>4</sub> fluxes, R<sub>eco</sub> and NEE exhibited a parabolic curve against the inundation depth (Fig. 4). Compared to the control, inundation significantly increased CH<sub>4</sub> fluxes ( $P < 0.05$ ), but affected CH<sub>4</sub> fluxes from 10 to 40 cm inundation depth to a minor degree (Fig. 3a and b). Inundation significantly increased R<sub>eco</sub> in both years relative to the control ( $P < 0.05$ ), except for 0 cm inundation depth, while only minor differences in R<sub>eco</sub> were found from 5 to 40 cm inundation depth in 2018, and among 5, 20, 30 and 40 cm inundation depth in 2019 (Fig. 3c and d). Inundation significantly increased NEE during the growing season in both years ( $P < 0.05$ ). However, inundation depth had little effect on NEE among 5, 10 and 20 cm inundation depth in 2018, and among 5, 10, 20, 30 and 40 cm inundation depth in 2019 (Fig. 3e and f). In addition, the CH<sub>4</sub> fluxes in 2018 were higher than those in 2019, whereas R<sub>eco</sub> and NEE in 2018 were lower than those in 2019 ( $P < 0.001$ ; Table 1). The inundation depth of 40 cm

had the highest, albeit still negative, GWP and the inundation depth of 5 cm resulted in the lowest GWP (closely followed by 10 cm) during the growing season in 2018, while there was little difference in GWP among the other inundation depths (Fig. 5a). During the growing season in 2019, inundation significantly decreased GWP compared to the control. However, only minor differences in GWP were found from 5 to 40 cm inundation depths, which overall decreased with increasing inundation depth (Fig. 5b). Our study also showed that NEE was the largest contributor to total seasonal GWP during the growing season in the Yellow River Delta (Table S1). In addition, the GWP in 2018 was much lower than that in 2019 (Fig. 5).

#### Relationships between ecosystem CO<sub>2</sub> and CH<sub>4</sub> exchange and WLAI, WHeight, and biomass

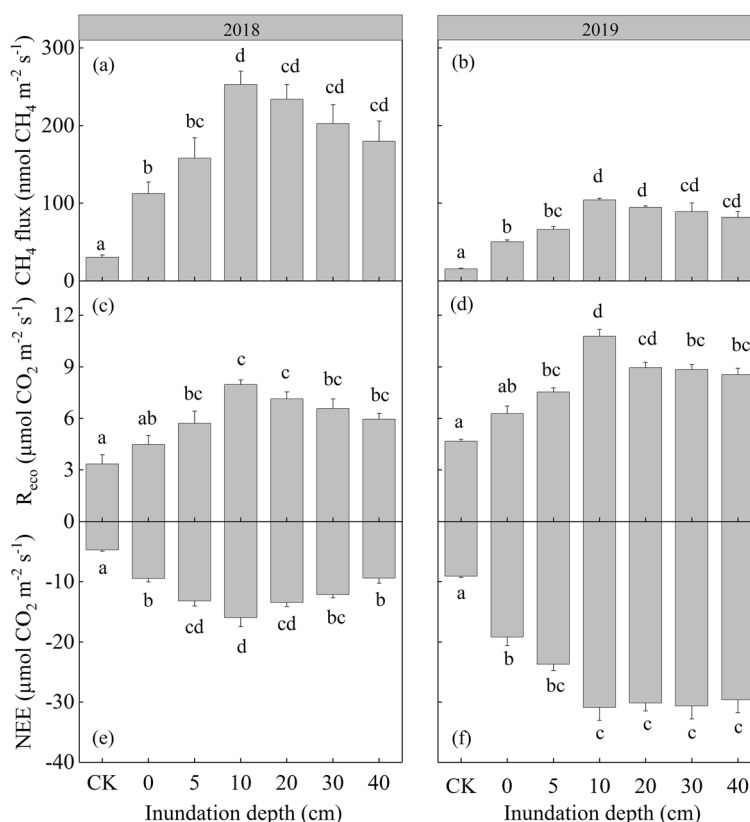
NEE was negatively, and R<sub>eco</sub> was positively correlated with the WLAI under different inundation depths during the growing season in 2018 and 2019 ( $P < 0.05$ ), whereas there was no significant relationship between CH<sub>4</sub> fluxes and WLAI (Fig. 6). Additionally, CH<sub>4</sub> fluxes, R<sub>eco</sub> and NEE were significantly related to WHeight during the growing season in both years (Fig. 7). CH<sub>4</sub> fluxes and R<sub>eco</sub> showed a weak, but significant, positive correlation with AGB in both years (Fig. 8a–g), while BGB was only positively correlated with CH<sub>4</sub> fluxes in 2018 (Fig. 8b). NEE had a weak, but significant, negative correlation with AGB, but only in 2018 (Fig. 8k).

## Discussion

### Effects of inundation depth on plant growth

Inundation regime is regarded an important hydrological factor affecting plant species diversity and

**Fig. 3** Variations in (a, b) CH<sub>4</sub> fluxes, (c, d) ecosystem respiration (R<sub>eco</sub>) and (e, f) net ecosystem CO<sub>2</sub> exchange (NEE) at different inundation depths during the growing season in 2018 and 2019 (means ± SE, n = 4). Different letters indicate significant differences between inundation depths (P < 0.05)



productivity in wetland ecosystems (Schile et al. 2011; Liu et al. 2018). In order to avoid the adverse effects of inundation, inundation-tolerant plants, such as *P. australis*, elongate their shoots to escape from submergence and restore leaf contact with the atmosphere (Striker et al. 2012; Voeselek et al. 2006). In the present study, inundation significantly increased WHeight of *P. australis* (Fig. 1), which indicated an escape strategy to cope with inundation. Meanwhile, inundation significantly increased shoot density, WLAI and biomass production (Figs. 1 and 2), suggesting that more energy and carbohydrates produced by photosynthesis will supplement the growth for plants to tolerate deep and long-lasting inundation (Chen et al. 2019). Additionally, BGB plays an important role in the accumulation of organic carbon in wetland ecosystems (Tripathee and Schäfer 2015). About 59 and 61% of the biomass of *P. australis* was allocated below ground under the different inundation depth. This suggests that a large part of the soil organic C may derive from roots, which will benefit long-term carbon sequestration under anaerobic conditions. Although many wetland plants can tolerate inundation, a situation in which inundation exceeds

plant tolerance is not beneficial to plant growth (Xue et al. 2018). For example, plant biomass of *Bolboschoenus planiculmis* was inhibited when inundation exceeded 10 cm inundation depth (An et al. 2018). Also, more than 91 cm inundation depth significantly decreased the leaf, belowground and total biomass of *Typha domingensis* (Chen et al. 2010). However, inundation depth had little effect on biomass in either of the investigated years (Fig. 2), which indicated that *P. australis* is tolerant to a broad range of inundation conditions.

#### Effects of inundation depth on ecosystem CH<sub>4</sub> fluxes

An increase in inundation depth significantly increased ecosystem CH<sub>4</sub> fluxes compared to the control during the growing season in 2018 and 2019 (Fig. 3a and b). For the soil CH<sub>4</sub> fluxes (Fig. S4b), inundation depth (0 cm) significantly increased soil CH<sub>4</sub> fluxes compared to the control due to anaerobic conditions which usually enhance CH<sub>4</sub> production by improving anaerobic decomposition by methanogenic bacteria and limiting CH<sub>4</sub> oxidation in reductive conditions (Kettunen et al.



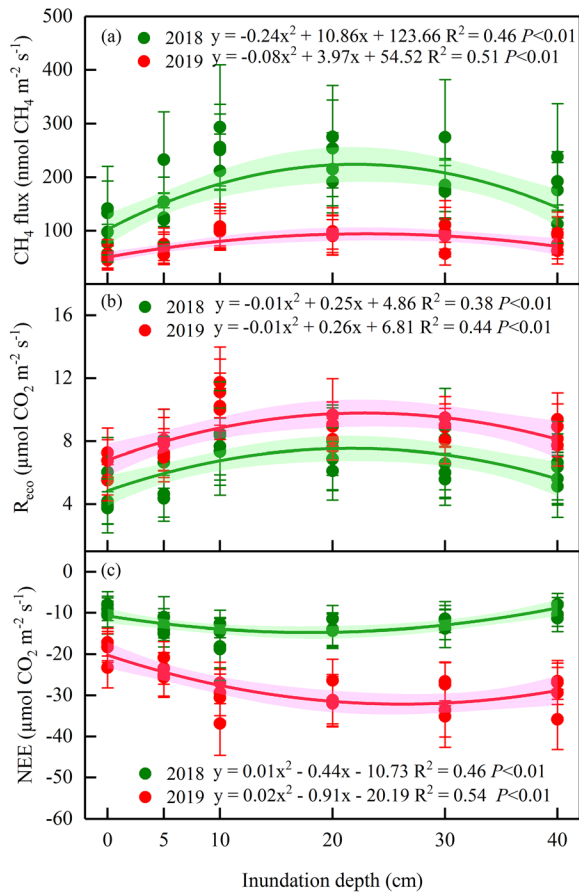


**Fig. 4** Relationships between (a) CH<sub>4</sub> fluxes, (b) ecosystem respiration ( $R_{\text{cco}}$ ) or (c) net ecosystem CO<sub>2</sub> exchange (NEE) and inundation depths in 2018 and 2019

1999). Other studies showed that inundation could have little effect on CH<sub>4</sub> fluxes as the water column can provide a diffusion barrier to the release of CH<sub>4</sub> from the soil or water (Cheng et al. 2007; Li et al. 2018; Wei et al. 2020). Moreover, growth of wetland plants (e.g. *P. australis*) affects soil redox conditions, resulting in increased CH<sub>4</sub> oxidation surrounding the rhizosphere due to enhanced turnover of root material and oxygen release (Colmer 2003; Chen et al. 2013). The above-ground and below-ground biomass at 5 cm to 40 cm inundation depths were larger than in the control (Fig. 2), which is likely to have resulted in more oxygen exudation to the surrounding rhizosphere. Thus, the more CH<sub>4</sub> was oxidized, the less soil CH<sub>4</sub> emissions under 5 to 40 cm inundation depths. Additionally, a small part of soil CH<sub>4</sub> could have been oxidized when passing through the water column (Boon and Lee 1997; Peacock et al. 2017). Thus, inundation depths from 5 to

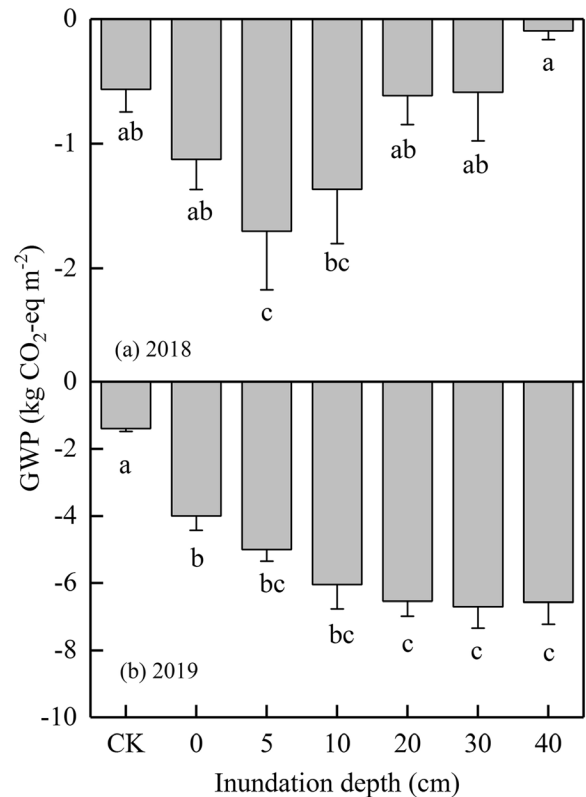


**Fig. 5** Variations in global warming potential (GWP) under different inundation depths during the growing season in (a) 2018 and (b) 2019 (means  $\pm$  SE,  $n = 4$ ). Different letters indicate significant differences between inundation depths ( $P < 0.05$ )

40 cm probably limited soil CH<sub>4</sub> fluxes. Our study showed that ecosystem CH<sub>4</sub> fluxes were much higher than soil CH<sub>4</sub> fluxes in our experiment (Fig. 3 and S4), which indicate that soil CH<sub>4</sub> fluxes contribute little to ecosystem CH<sub>4</sub> fluxes. Although inundation depth limited soil CH<sub>4</sub> fluxes, inundation depth increased the ecosystem CH<sub>4</sub> fluxes compared to the control, which may partly be due to the increased shoot density, WHeight, and biomass (Fig. 1a-d, Fig. 7a and b, Fig. 8a-c).

Increased vascular plant height, shoot density and biomass would increase CH<sub>4</sub> emissions due to higher plant productivity (Fischer et al. 2010; Jeffrey et al. 2019). Previous studies have demonstrated that plant productivity is a good predictor of CH<sub>4</sub> fluxes across a wide range of wetlands (Chen et al. 2009; Fischer et al. 2010; Mozdzer and Megonigal 2013; Sun et al. 2018; Li et al. 2019). In our plots, the vegetation is relatively homogeneous and mostly dominated by *Phragmites*

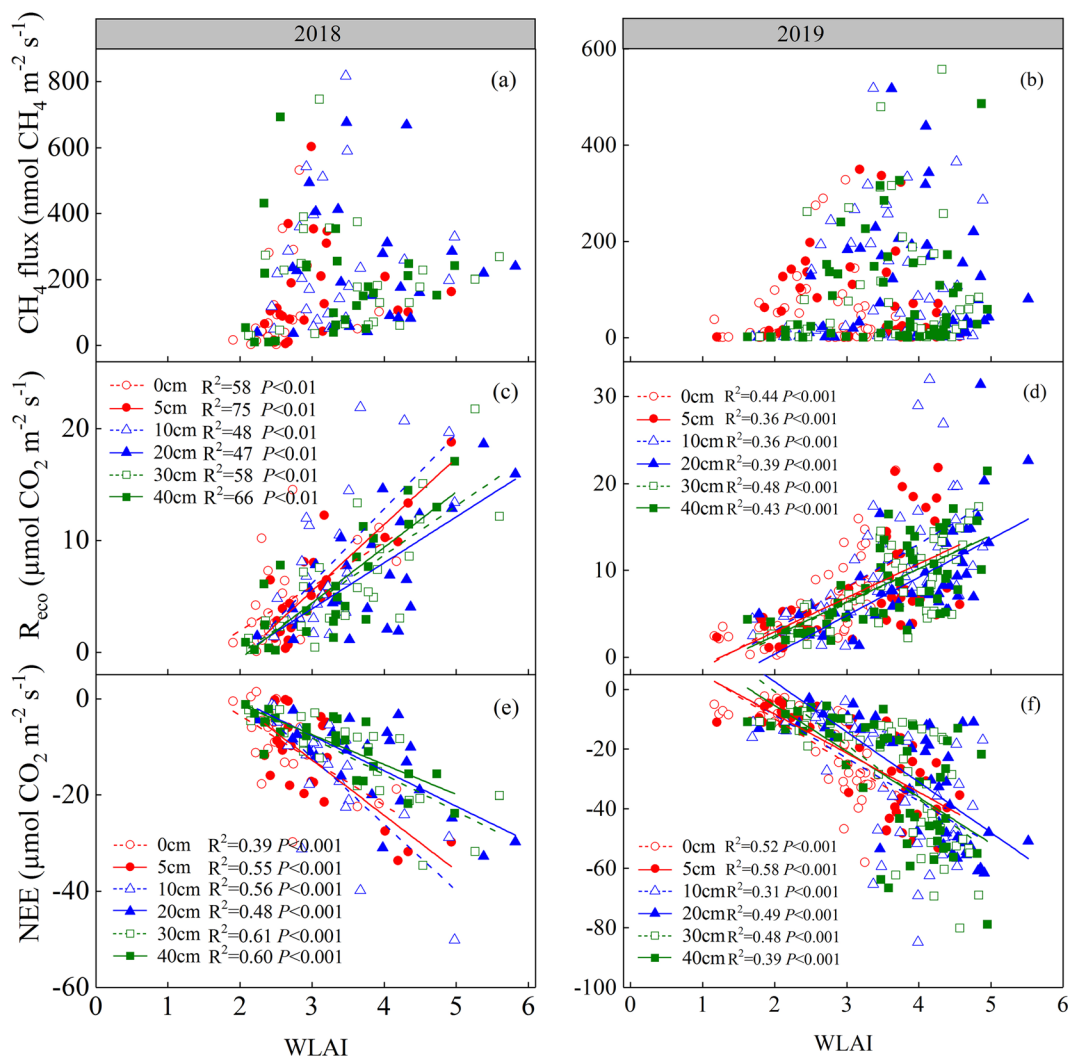
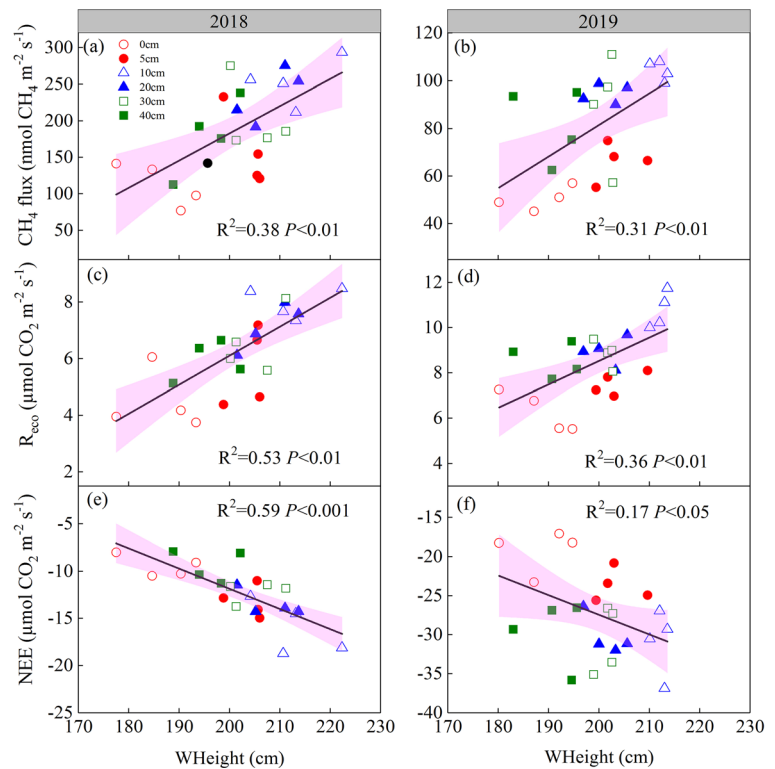


**Fig. 6** Relationships between (a, b)  $\text{CH}_4$  fluxes, (c, d) ecosystem respiration ( $R_{\text{eco}}$ ) and (e, f) net ecosystem  $\text{CO}_2$  exchange (NEE) in response to above-water level leaf area index (WLAI) under different inundation depths during the growing season in 2018 and 2019

*australis*, an inundation-tolerant vascular plant. Also, a significant linear relationship was found between  $\text{CH}_4$  fluxes and WHeight or biomass (Fig. 7a and b, Fig. 8a-c). On the one hand, higher plant productivity could capture more atmospheric  $\text{CO}_2$  and increase the production of C substrates available for methanogenesis and can thus lead to higher  $\text{CH}_4$  production (Li et al. 2019; Cheng et al. 2007; Koelbener et al. 2010). On the other hand, the more plant biomass is produced under inundated conditions, the more aerenchyma conduits are present, suggesting that more  $\text{CH}_4$  could bypass from the anaerobic zone to the atmosphere (Henneberg et al.

2012; Bridgham et al. 2013). This is consistent with studies in other wetlands (Chen et al. 2009; Fischer et al. 2010; Mozdzer and Megonigal 2013; Minke et al. 2016), which indicated that vascular plants play an important role in  $\text{CH}_4$  emissions in wetland ecosystems when water levels are above the soil surface in coastal wetlands (Bridgham et al. 2013). However, there was no significant difference in  $\text{CH}_4$  fluxes from 10 to 40 cm inundation depth (Fig. 3a and b), which was probably because inundation depth from 10 to 40 cm had no effect on shoot density and biomass (Figs. 1a and b, and 2). We also found that  $\text{CH}_4$  fluxes in 2018 were higher than

**Fig. 7** Relationships between (a, b) CH<sub>4</sub> fluxes, (c, d) ecosystem respiration (R<sub>eco</sub>) and (e, f) net ecosystem CO<sub>2</sub> exchange (NEE) in response to plant height relative to water level (WHeight) under different inundation depths during the growing season in 2018 and 2019. The black lines are fitted regressions, and the light pink-shaded areas around the regression lines are 95% confidence intervals



those in 2019 ( $P < 0.05$ , Fig. 3a and b), which was probably related to redox conditions. Under anaerobic conditions, anaerobic oxidation of methane may consume 200 Tg CH<sub>4</sub> per year in global wetland, decreasing the potential CH<sub>4</sub> emissions by over 50% (Segarra et al. 2015). Since wetland plants (e.g. *P. australis*) could transport oxygen to rhizospheres and sediments, their presence will reduce CH<sub>4</sub> concentrations (Jeffrey et al. 2019). Previous studies showed that CH<sub>4</sub> emissions were negatively related to plant biomass, which was often attributed to an increased rhizospheric oxygenation and CH<sub>4</sub> consumption by rhizospheric bacteria (Bhullar et al. 2013; Kao-Kniffin et al. 2010). In our study, the mean BGB in 2019 (2434 g m<sup>-2</sup>) was higher than in 2018 (2318 g m<sup>-2</sup>), which means that in 2019 more CH<sub>4</sub> was oxidized to a certain degree. Additionally, the CH<sub>4</sub> fluxes reached a peak in August (Fig. S3a and b), mainly because the density and WHeight reached a peak in August (Fig. S2a-d). Our study also demonstrated a clearly parabolic response of CH<sub>4</sub> fluxes to the gradient of inundation depth (Fig. 4a), which was not observed in previous studies (Chen et al. 2009; Minke et al. 2016). There are

several potential mechanisms that could have contributed to this relationship. Firstly, an increase in inundation depth from 0 to 5 cm promoted an increase in CH<sub>4</sub> fluxes during the growing season, which is partly mainly because of increased plant traits with increasing inundation depth. Meanwhile, a significant positive linear correlation between WHeight and CH<sub>4</sub> fluxes was found (Fig. 7a and b), suggesting that the higher the WHeight, the more CH<sub>4</sub> emissions. Secondly, a large part of the CH<sub>4</sub> emissions in *P. australis* occurs close to the ground (Van Der Nat et al. 1998). For example, in a brackish-water tidal marsh of China, the main part of *P. australis* CH<sub>4</sub> emissions is in the base of plant, especially at a height of 0–20 cm above the ground (Tong et al. 2012). In a boreal lake, CH<sub>4</sub> probably escaped through the lower part of *P. australis* (<10 cm above the sediment surface) because the lacunal CH<sub>4</sub> concentrations were highest here (Käki et al. 2001). Inundation depth (20 to 40 cm) could inhibit the path of CH<sub>4</sub> emissions through the submerged plant shoots and cause a decline in CH<sub>4</sub> emissions. Thus, the higher WHeight was accompanied by higher CH<sub>4</sub> fluxes at 10 cm inundation

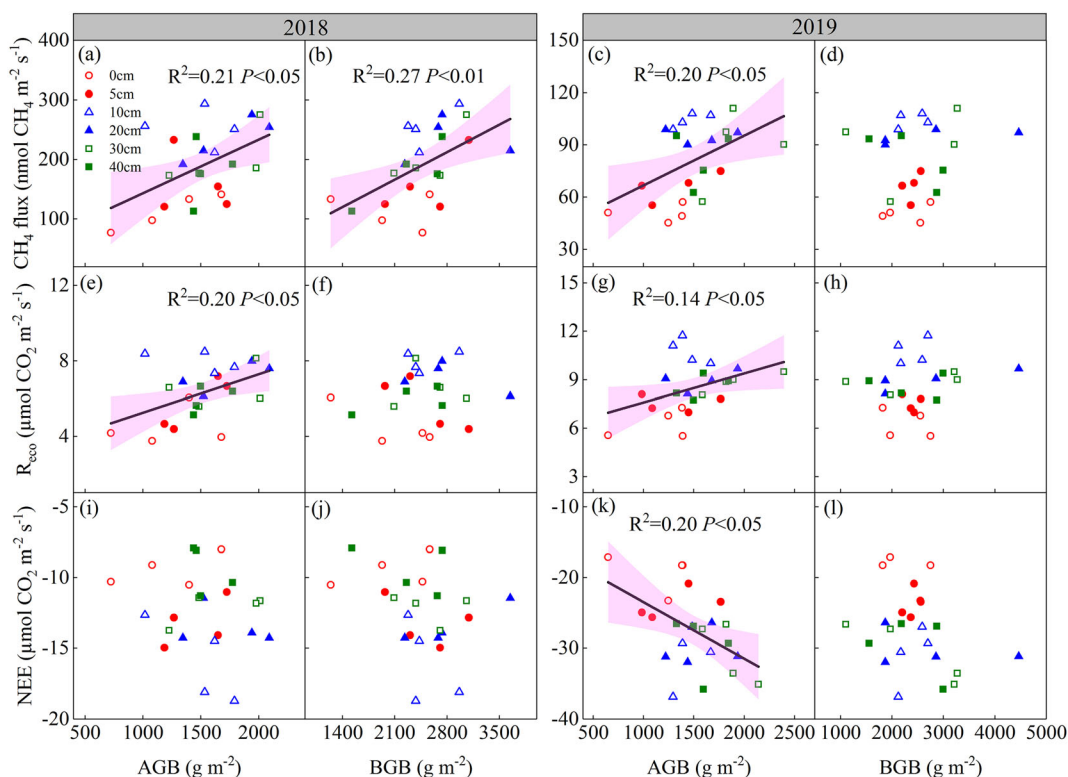


**Fig. 8** Relationships between (a, b, c, d) CH<sub>4</sub> fluxes, (e, f, g, h) ecosystem respiration ( $R_{eco}$ ) and (i, j, k, l) net ecosystem CO<sub>2</sub> exchange (NEE) in response to (a, c, e, g, i, k) aboveground biomass (AGB) and (b, d, f, h, j, l) belowground biomass

(BGB) under different inundation depths during the growing season in 2018 and 2019. The black lines are fitted regressions, and the light pink-shaded areas around the regression lines are 95% confidence

depth, but at inundation depths from 20 to 40 cm CH<sub>4</sub> fluxes declined to a certain degree.

#### Effects of inundation depth on ecosystem CO<sub>2</sub> exchange

During the growing season in 2018 and 2019, the  $R_{eco}$  and NEE showed an increase as inundation depth increased compared to the control (Fig. 3c-f), which was correlated with increased WLAI, WHeight and AGB (Figs. 6c-f, 7c-f, 8e-k). The plant parts below water level had little effect on  $R_{eco}$  and NEE because the plant respiration and uptake of CO<sub>2</sub> for photosynthesis were limited (Jimenez et al. 2012). Thus, especially plant parts above water level are important for the ecosystem CO<sub>2</sub> exchange in wetland ecosystems. Plant respiration is tightly coupled to C input from the above-water level photosynthesis (Song et al. 2011; Han et al. 2012). The leaf area determines the amount of available photosynthate and the amount of light being intercepted by the vegetation, therefore the increased WLAI could enhance the uptake of CO<sub>2</sub> for photosynthesis on an ecosystem

level (Wang et al. 2016; Acosta et al. 2017). Thus, the difference in WLAI caused by inundation depth may have been an important plant-related factor leading to the variation in  $R_{eco}$  and NEE (Han et al. 2012; Song et al. 2011). The significant correlations between  $R_{eco}$  and NEE and plant traits indicate that biotic factors are important for regulating CO<sub>2</sub> exchange in wetland ecosystems (Han et al. 2014; Minke et al. 2016). For example, in an Amazon floodplain wetland, NEE was increased by 20% under high water (inundated) compared to low water level, which was attributed to the higher living biomass (Morison et al. 2000). In a temperate cutover fen,  $R_{eco}$  and NEE significant increased with increasing inundation depth from 0 to 100 cm mainly due to the increased AGB (Minke et al. 2016). Previous studies reported opposite results indicating that inundation decreased  $R_{eco}$  and NEE in wetland ecosystems (Han et al. 2015; Zhao et al. 2019). The submerged plant shoots and leaves showed a reduction in the photosynthetic rates and plant respiration (Jimenez et al. 2012). In addition, the reduced  $R_{eco}$  under inundation

conditions was mainly due to the saturation of soils, subsequent oxygen limitation, and inhibition of root and soil respiration that led to lower CO<sub>2</sub> emissions (Han et al. 2015). However, the ecosystem CO<sub>2</sub> exchange can vary between different plant species. For example, Zhao et al. (2019) observed a decline in R<sub>eco</sub> and NEE as inundation depth increased from 0 to 45.6 cm in a freshwater wetland dominated by sawgrass (*Cladium jamaicense* Crantz) and muhly grass (*Muhlenbergia filipes* M.A. Curtis), a weak inundation-tolerant plant. On the contrary, inundation depth (from 0 to 24 cm) enhanced R<sub>eco</sub> and NEE of *Spartina alterniflora*, a stronger inundation tolerant plant (Jones et al. 2018). Therefore, the effect of inundation depth on different plant species needs to be considered in wetland ecosystems. However, there was no significant differences in R<sub>eco</sub> were found from 5 to 40 cm inundation depth in 2018, among 5, 20, 30 and 40 cm inundation depth in 2019, no differences in NEE among 5, 10 and 20 cm inundation depth in 2018, and from 5 to 40 cm inundation depth in 2019 (Fig. 3c-f), which mainly due to inundation depth had little effect on plant productivity among 5 to 40 cm inundation depth (Figs. 1 and 2). Additionally, WLAI, as discussed above, plays a very important role in ecosystem CO<sub>2</sub> exchange. Mean WLAI values under different inundation depths in 2018 (3.26) were lower than those in 2019 (3.42) ( $P < 0.05$ ; Table 1), which probably resulted in lower R<sub>eco</sub> and NEE in 2018 than in 2019 ( $P < 0.05$ , Fig. 3c and f). We also found the R<sub>eco</sub> and NEE reached a peak in July (Fig. S3c-f), which was mainly due to the peak of WLAI in July (Fig. S2e-f). R<sub>eco</sub> and NEE exhibited a parabolic pattern against the inundation depth (Fig. 4b and c) and this nonlinear relationship has not often been reported before (Zhao et al. 2019). The majority of previous studies have only compared situations with and without inundation (Han et al. 2015; Sánchez-Rodríguez et al. 2019), but there were few studies on the effect of different inundation depths on ecosystem CO<sub>2</sub> exchange. In this study, we spanned a large range of inundation depths, to be able to observe a continuous response of R<sub>eco</sub> and NEE to different inundation depths. We found parabolic relationship responses of R<sub>eco</sub> and NEE to different inundation depths, which are likely to be induced by nonlinear changes in plant productivity. As mentioned above, the vegetation parts above water level could be important for ecosystem CO<sub>2</sub> exchange under different inundation depths. On the one hand, the higher the WHeight and WLAI, the higher the

absorption capacity of light, the higher the uptake of CO<sub>2</sub> for photosynthesis and the higher plant respiration. On the other hand, the deeper the inundation (20, 30 and 40 cm), the more plant shoots and leaves were submerged, which resulted in a partial plant stomatal closure under water and a lower photosynthesis activity of submerged leaves (Schedlbauer et al. 2010; Han et al. 2015). Moreover, due to the slow diffusion rate of CO<sub>2</sub> in water, the diffusive boundary layer resistance could limit CO<sub>2</sub> emission through the water surface (Han et al. 2015). Meanwhile, CO<sub>2</sub> gas can dissolve in water, which suggested that the deeper the inundation, the less CO<sub>2</sub> efflux from water columns (Leopold et al. 2016). As a result, the R<sub>eco</sub> and NEE decreased with the increase of inundation depth from 20 to 40 cm. Contrary to our results, R<sub>eco</sub> and NEE linearly decreased with increasing water level from 0 to 45.6 cm in a freshwater wetland where the height of the vegetation was about 73 cm (Zhao et al. 2019). This is probably due to the fact that plant height above water level linearly decreased with the increase in water level.

Additionally, inundation depth decreased the GWP during the growing season compared to the control (Fig. 5), which suggested that relatively shallow inundation depths (5 cm in 2018 and all inundation treatments in 2019) were efficient in mitigating GHG emissions in the studied coastal wetland. The negative GWP under different inundation depths indicated that NEE was the largest contributor to the seasonal GWP, mainly because NEE values were much higher than the sum of CH<sub>4</sub> and R<sub>eco</sub> (Table S1). Similar results have also been found in a freshwater marshland (Zhang et al. 2013) and restored deltaic wetland (Hemes et al. 2019). We also found that GWP varied greatly between 2018 and 2019, which was consistent with the results in a restored deltaic wetland (Hemes et al. 2019). This variation was due to the fact that the ecosystem C exchange showed significant differences between years. In our experiment, only the GWP of CO<sub>2</sub> and CH<sub>4</sub> fluxes were calculated, N<sub>2</sub>O fluxes were not included. Therefore, long-term observations of all three GHGs are essential to evaluate the GWP and to better quantify wetland C sources and sinks.

#### Limitation of the research and outlook

Inundation depth strongly altered ecosystem CH<sub>4</sub> and CO<sub>2</sub> exchange, which was coincident with affected shoot density, height, leaf area index and biomass of

*P. australis*. However, the effects of abiotic factors (e.g. soil redox conditions, substrate and dissolved organic carbon) on ecosystem C exchange (especially CH<sub>4</sub> emissions) were not considered in our study. Meanwhile, we did not reinforce the impact of inundation duration and frequency on the C sink-source status. These limitations will increase the uncertainty about the effect of inundation regimes on ecosystem CH<sub>4</sub> and CO<sub>2</sub> exchange in freshwater wetlands in the Yellow River Estuary. Hence, future field and long-term continuous data are required to improve our knowledge on the potential impacts of hydrological regimes (inundation depth, frequency and duration) on C sequestration in wetland ecosystems.

## Conclusions

This study demonstrated that ecosystem CH<sub>4</sub> and CO<sub>2</sub> exchange (CH<sub>4</sub> fluxes, R<sub>eco</sub> and NEE) increased with increasing inundation depth in a freshwater wetland in the Yellow River Estuary, which could partly be due to the increased plant productivity (e.g. shoot density, above-water level leaf area index, plant height relative to water level and biomass) during the growing season. However, there were only minor differences in CH<sub>4</sub> fluxes, R<sub>eco</sub> or NEE between inundation depths ranging from 10 to 40 cm, especially in 2019. The CH<sub>4</sub> fluxes, R<sub>eco</sub> or NEE exhibited parabolic responses to inundation depth, which correlated with changing plant traits under different inundation depths. In addition, NEE was the largest contributor to total seasonal global warming potential under different inundation depths during the growing season. To understand the responses of ecosystem CH<sub>4</sub> and CO<sub>2</sub> exchange to inundation depth is important for accurately improving the ecosystem C model and it also helpful to predict the ecosystem carbon sinks or sources under the changing hydrological regimes with respect to climate change.

**Acknowledgements** This research was jointly funded by a Strategic Priority Research Program of the Chinese Academy of Sciences (XDA23050202), a National Nature Science Foundation of China project (41671089, 41977186), a Forestry Science and Technology Innovation Project of Shandong Province (2019LY006), and a Chongqing Research Program of Basic Research and Frontier Technology (cstc2018jcyjAX0476). We are grateful for the support from Yellow River Delta Ecological Research Station of Coastal Wetland, the Chinese Academy of Sciences.

## References

- Acosta M, Juszczak R, Chojnicki B, Pavelka M, Havránková K, Lesny J, Krupková L, Urbaniak M, Macháčová K, Olejnik J (2017) CO<sub>2</sub> fluxes from different vegetation communities on a peatland ecosystem. *Wetlands* 37:423–435
- An Y, Gao Y, Tong S (2018) Emergence and growth performance of *Bolboschoenus planiculmis* varied in response to water level and soil planting depth: implications for wetland restoration using tuber transplantation. *Aquat Bot* 148:10–14
- Bhullar GS, Iravani M, Edwards PJ, Venterink HO (2013) Methane transport and emissions from soil as affected by water table and vascular plants. *BMC Ecol* 13:32
- Boon PI, Lee K (1997) Methane oxidation in sediments of a floodplain wetland in South-Eastern Australia. *Lett Appl Microbiol* 25:138–142
- Bridgman SD, Cadillo-Quiroz H, Keller JK, Zhuang Q (2013) Methane emissions from wetlands: biogeochemical, microbial, and modeling perspectives from local to global scales. *Glob Chang Biol* 19:1325–1346
- Chen H, Wu N, Yao S, Gao Y, Dan Z, Wang Y, Xiong W, Yuan X (2009) High methane emissions from a littoral zone on the Qinghai-Tibetan plateau. *Atmos Environ* 43:4995–5000
- Chen HJ, Zamorano MF, Ivanoff D (2010) Effect of flooding depth on growth, biomass, photosynthesis, and chlorophyll fluorescence of *Typha domingensis*. *Wetlands* 30:957–965
- Chen H, Zhu Q, Peng C, Wu N, Wang Y, Fang X, Jiang H, Xiang W, Chang J, Deng X, Yu G (2013) Methane emissions from rice paddies natural wetlands, lakes in China: synthesis new estimate. *Glob Chang Biol* 19:19–32
- Chen X-S, Li Y-F, Cai Y-H, Xie Y-H, Deng Z-M, Li F, Hou Z-Y (2019) Differential strategies to tolerate flooding in *Polygonum hydropiper* plants originating from low-and high-elevation habitats. *Front Plant Sci* 9:1970
- Cheng X, Peng R, Chen J, Luo Y, Zhang Q, An S, Chen J, Li B (2007) CH<sub>4</sub> and N<sub>2</sub>O emissions from *Spartina alterniflora* and *Phragmites australis* in experimental mesocosms. *Chemosphere* 68:420–427
- Colmer TD (2003) Long-distance transport of gases in plants: a perspective on internal aeration and radial oxygen loss from roots. *Plant Cell Environ* 26:17–36
- Fischer JCV, Rhew RC, Ames GM, Fosdick BK, Fischer PEV (2010) Vegetation height and other controls of spatial variability in methane emissions from the Arctic coastal tundra at Barrow, Alaska. *J Geophys Res* 115:G00103
- Garssen AG, Baattrup-Pedersen A, Voesenek LACJ, Verhoeven JTA, Soons MB (2015) Riparian plant community responses to increased flooding: a meta-analysis. *Glob Chang Biol* 21:2881–2890
- Han G, Yang L, Yu J, Wang G, Miao P, Gao Y (2012) Environmental controls on net ecosystem CO<sub>2</sub> exchange over a reed (*Phragmites australis*) wetland in the Yellow River Delta, China. *Estuar Coast* 36:401–413
- Han G, Xing Q, Yu J, Luo Y, Li D, Yang L, Wang G, Miao P, Xie B, Mickle N (2014) Agricultural reclamation effects on ecosystem CO<sub>2</sub> exchange of a coastal wetland in the Yellow River Delta. *Agric Ecosyst Environ* 196:187–198
- Han G, Chu X, Xing Q, Li D, Yu J, Luo Y, Wang G, Miao P, Rafique R (2015) Effects of episodic flooding on the net

- ecosystem CO<sub>2</sub> exchange of a supratidal wetland in the yellow river delta. *J Geophys Res-Biogeog* 120:1506–1520
- Han G, Sun B, Chu X, Xing Q, Song W, Xia J (2018) Precipitation events reduce soil respiration in a coastal wetland based on four-year continuous field measurements. *Agric For Meteorol* 256:292–303
- Hemes KS, Chamberlain SD, Eichelmann E, Anthony T, Valach A, Kasak K, Szutu D, Verfaillie J, Silver WL, Baldocchi DD (2019) Assessing the carbon and climate benefit of restoring degraded agricultural peat soils to managed wetlands. *Agric For Meteorol* 268:202–214
- Henneberg A, Sorrell BK, Brix H (2012) Internal methane transport through *Juncus effusus*: experimental manipulation of morphological barriers to test above- and below-ground diffusion limitation. *New Phytol* 196:799–806
- IPCC (2013) Climate change 2013: the physical science basis. Contributions of working group I to the fifth assessment report of the intergovernmental panel on climate change. NY, New York
- Jeffrey LC, Maher DT, Johnston SG, Kelaher BP, Steven A, Tait DR (2019) Wetland methane emissions dominated by plant-mediated fluxes: contrasting emissions pathways and seasons within a shallow freshwater subtropical wetland. *Limnol Oceanogr* 64:1895–1912
- Jimenez KL, Starr G, Staudhammer CL, Schedlbauer JL, Loescher HW, Malone SL, Oberbauer SF (2012) Carbon dioxide exchange rates from short-and long-hydroperiod everglades freshwater marsh. *J Geophys Res-Atmos* 117(G4)
- Jones SF, Stagg CL, Krauss KW, Hester MW (2018) Flooding alters plant-mediated carbon cycling independently of elevated atmospheric CO<sub>2</sub> concentrations. *J Geophys Res-Biogeog* 123:1976–1987
- Jungkunst HF, Fiedler S (2007) Latitudinal differentiated water table control of carbon dioxide, methane and nitrous oxide fluxes from hydromorphic soils: feedbacks to climate change. *Glob Chang Biol* 13:2668–2683
- Käki T, Ojala A, Kankaala P (2001) Diel variation in methane emissions from stands of *Phragmites australis* (Cav.) Trin. ex Steud. and *Typha latifolia* L. in a boreal lake. *Aquat Bot* 71: 259–271
- Kao-Kniffin J, Freyre DS, Balsler TC (2010) Methane dynamics across wetland plant species. *Aquat Bot* 93:107–113
- Kettunen A, Kaitala V, Lethinen A, Lohila A, Alm J, Silvola J, Martikainen PJ (1999) Methane production and oxidation potentials in relation to water table fluctuations in two boreal mires. *Soil Biol Biochem* 31:1741–1749
- Koelbener A, Ström L, Edwards PJ, Venterink HO (2010) Plant species from mesotrophic wetlands cause relatively high methane emissions from peat soil. *Plant Soil* 326:147–158
- Leopold A, Marchand C, Renchon A, Deborde J, Quiniou T, Allenbach M (2016) Net ecosystem CO exchange in the “Coeur de Voh” mangrove, New Caledonia: effects of water stress on mangrove productivity in a semi-arid climate. *Agr Forest Meteorol* 223:217–232
- Li H, Dai S, Ouyang Z, Xie X, Guo H, Gu C, Xiao X, Ge Z, Peng C, Zhao B (2018) Multi-scale temporal variation of methane flux and its controls in a subtropical tidal salt marsh in eastern China. *Biogeochemistry* 137:163–179
- Li H, Guo H, Helbig M, Dai S, Zhang M, Zhao M, Peng C, Xiao X, Zhao B (2019) Does direct-seeded rice decrease ecosystem-scale methane emissions? — a case study from a rice paddy in Southeast China. *Agric For Meteorol* 272-273: 118–127
- Liu Y, Ding Z, Bachofen C, Lou Y, Jiang M, Tang X, Lu X, Buchmann N (2018) The effect of saline-alkaline and water stresses on water use efficiency and standing biomass of *Phragmites australis* and *Bolboschoenus planiculmis*. *Sci Total Environ* 644:207–216
- Matsuda Y, Hopkinson BM, Nakajima K, Dupont CL, Tsuji Y (2017) Mechanisms of carbon dioxide acquisition and CO<sub>2</sub> sensing in marine diatoms: a gateway to carbon metabolism. *Philos Trans R Soc Lond* 372:20160403
- McNicol G, Silver WL (2014) Separate effects of flooding and anaerobiosis on soil greenhouse gas emissions and redox sensitive biogeochemistry. *J Geophys Res-Biogeog* 119: 557–566
- Minke M, Augustin J, Burlo A, Yarmashuk T, Chuvashova H, Thiele A, Freibauer A, Tikhonov V, Hoffmann M (2016) Water level, vegetation composition, and plant productivity explain greenhouse gas fluxes in temperate cutover fens after inundation. *Biogeosciences* 13:3945–3970
- Mitsch WJ, Gosselink JG (2007) Wetlands, 4th edn. Wiley, Hoboken
- Morison JIL, Piedade MTF, Müller E, Long SP, Junk WJ, Jones MB (2000) Very high productivity of the C<sub>4</sub> aquatic grass *Echinochloa polystachya* in the Amazon floodplain confirmed by net ecosystem CO<sub>2</sub> flux measurements. *Oecologia* 125(3):400–411
- Mozdzer TJ, Megonigal JP (2013) Increased methane emissions by an introduced *Phragmites australis* lineage under global change. *Wetlands* 33:609–615
- Nahlik AM, Fennessy MS (2016) Carbon storage in US wetlands. *Nat Commun* 7:13835
- Olefeldt D, Euskirchen ES, Harden J, Kane E, McGuire AD, Waldrop MP, Turetsky MR (2017) A decade of boreal rich fen greenhouse gas fluxes in response to natural and experimental water table variability. *Glob Chang Biol* 23:2428–2440
- Peacock M, Ridley LM, Evans CD, Gauci V (2017) Management effects on greenhouse gas dynamics in fen ditches. *Sci Total Environ* 578:601–612
- Rasmussen TC, Deemy JB, Long SL (2018) Wetland hydrology. In: Finlayson C et al (eds) The wetland book. Springer, Dordrecht
- Ratcliffe JL, Campbell DI, Clarkson BR, Wall AM, Schipper LA (2019) Water table fluctuations control CO<sub>2</sub> exchange in wet and dry bogs through different mechanisms. *Sci Total Environ* 655:1037–1046
- Sairam RK, Kumutha D, Ezhilmathi K, Deshmukh PS, Srivastava GC (2008) Physiology and biochemistry of waterlogging tolerance in plants. *Biol Plant* 52(3):401–412
- Sánchez-Rodríguez AR, Nie CR, Hill PW, Chadwick DR, Jones DL (2019) Extreme flood events at higher temperatures exacerbate the loss of soil functionality and trace gas emissions in grassland. *Soil Biol Biochem* 130:227–236
- Schedlbauer JL, Oberbauer SF, Starr G, Jimenez KL (2010) Seasonal differences in the CO<sub>2</sub> exchange of a short-hydroperiod Florida Everglades marsh. *Agric For Meteorol* 150:994–1006
- Schile LM, Callaway JC, Parker T, Vasey MC (2011) Salinity and inundation influence productivity of the halophytic plant *Sarcocornia pacifica*. *Wetlands* 31:1165–1174

- Segarra KEA, Schubotz F, Samarkin V, Yoshinaga MY, Hinrichs K, Joye SB (2015) High rates of anaerobic methane oxidation in freshwater wetlands reduce potential atmospheric methane emissions. *Nat Commun* 61:7477
- Song C, Sun L, Huang Y, Wang Y, Wan Z (2011) Carbon exchange in a freshwater marsh in the Sanjiang plain, northeastern China. *Agric For Meteorol* 151:1131–1138
- Striker GG, Izaguirre RF, Manzur ME, Grimoldi AA (2012) Different strategies of *Lotus japonicus*, *L. corniculatus* and *L. tenuis* to deal with complete submergence at seedling stage. *Plant Biol* 14:50–55
- Sun L, Song C, Lafleur PM, Miao Y, Wang X, Gong C, Qiao T, Yu X, Tan W (2018) Wetland-atmosphere methane exchange in Northeast China: a comparison of permafrost peatland and freshwater wetlands. *Agric For Meteorol* 249:239–249
- Tian H, Chen G, Lu C, Xu X, Hayes DJ, Ren W, Pan S, Huntzinger DN, Wofsy SC (2015) North American terrestrial CO<sub>2</sub> uptake largely offset by CH<sub>4</sub> and N<sub>2</sub>O emissions: toward a full accounting of the greenhouse gas budget. *Clim Chang* 129:413–426
- Tong C, Huang J, Wang W, Liao J, Liu Z, Zeng C (2012) Methane dynamics of a brackish-water tidal *Phragmites australis* marsh in the Minjiang River estuary. *Acta Geograph Sin* 67(9):1165–1180 (in Chinese)
- Trenberth KE (2011) Changes in precipitation with climate change. *Clim Res* 47:123–138
- Tripathee R, Schäfer KVR (2015) Above- and belowground biomass allocation in four dominant salt marsh species of the eastern United States. *Wetlands* 35:21–30
- Van Der Nat F-JWA, Middelburg JJ, Meteren VD, Wielemakers A (1998) Diel methane emission patterns from *Scripus lacustris* and *Phragmites australis*. *Biogeochemistry* 41:1–22
- Voeselek LACJ, Colmer TD, Pierik R, Millenaar FF, Peeters AJM (2006) How plants cope with complete submergence. *New Phytol* 170:213–226
- Wang L, Liu H, Sun J, Shao Y (2016) Biophysical effects on the interannual variation in carbon dioxide exchange of an alpine meadow on the Tibetan plateau. *Atmos Chem Phys* 17:1–28
- Wang H, Yu L, Zhang Z, Liu W, Chen L, Cao G, Yue H, Zhou J, Yang Y, Tang Y, He J (2017) Molecular mechanisms of water table lowering and nitrogen deposition in affecting greenhouse gas emissions from a Tibetan alpine wetland. *Glob Chang Biol* 23:815–829
- Webb RH, Leake SA (2006) Ground-water surface-water interactions and long-term change in riverine riparian vegetation in the southwestern United States. *J Hydrol* 320:302–323
- Wei S, Han G, Chu X, Song W, He W, Xia J, Wu H (2020) Effect of tidal flooding on ecosystem CO<sub>2</sub> and CH<sub>4</sub> fluxes in a salt marsh in the Yellow River Delta. *Estuar Coast Shelf S* 232:106512
- Westra S, Fowler HJ, Evans JP, Alexander LV, Berg P, Johnson F, Kendon EJ, Lenderink G, Roberts NM (2014) Future changes to the intensity and frequency of short-duration extreme rainfall. *Rev Geophys* 52:522–555
- Xiao D, Deng L, Kim D, Huang C, Tian K (2019) Carbon budgets of wetland ecosystems in China. *Glob Chang Biol* 25:2061–2076
- Xue L, Li X, Yan Z, Zhang Q, Ding W, Huang X, Tian B, Ge Z, Yin Q (2018) Native and non-native halophytes resiliency against sea-level rise and saltwater intrusion. *Hydrobiologia* 806:47–65
- Yang J, Liu J, Hu X, Li X, Wang Y, Li H (2013) Effect of water table level on CO<sub>2</sub>, CH<sub>4</sub> and N<sub>2</sub>O emissions in a freshwater marsh of Northeast China. *Soil Biol Biochem* 61:52–60
- Yang G, Chen H, Wu N, Tian J, Peng C, Zhu Q, Zhu D, He Y, Zheng Q, Zhang C (2014) Effects of soil warming, rainfall reduction and water table level on CH<sub>4</sub> emissions from the Zoige peatland in China. *Soil Biol Biochem* 78:83–89
- Yang W, Li X, Sun T, Yang Z, Li M (2017) Habitat heterogeneity affects the efficacy of ecological restoration by freshwater releases in a recovering freshwater coastal wetland in China's Yellow River Delta. *Ecol Eng* 104:1–12
- Zhang L, Song C, Nkrumah PN (2013) Responses of ecosystem carbon dioxide exchange to nitrogen addition in a freshwater marshland in Sanjiang plain, Northeast China. *Environ Pollut* 180:55–62
- Zhao J, Oberbauer SF, Olivas PC, Schedlbauer JL, May JL, Moser JG, Malone SL, Staudhammer CL, Starr G (2018) Contrasting photosynthetic responses of two dominant macrophyte species to seasonal inundation in an Everglades freshwater prairie. *Wetlands* 38(5):893–903
- Zhao J, Malone SL, Oberbauer SF, Olivas PC, Schedlbauer JL, Staudhammer CL, Starr G (2019) Intensified inundation shifts a freshwater wetland from a CO<sub>2</sub> sink to a source. *Global Chang Biol* 25:3319–3333

**Publisher's note** Springer Nature remains neutral with regard to jurisdictional claims in published maps and institutional affiliations.